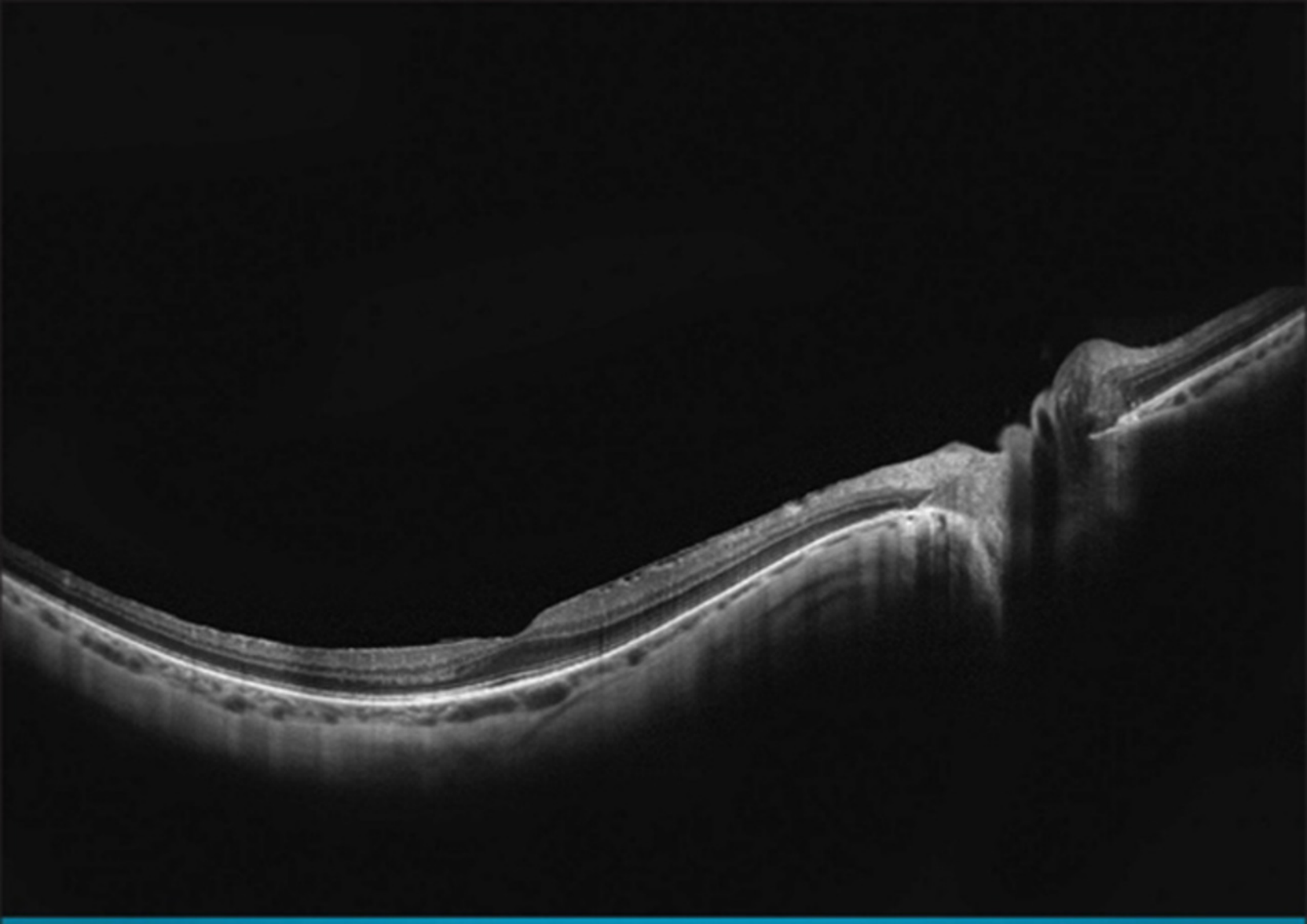

Atlas of Retinal OCT

Darin R. **Goldman**
Nadia K. **Waheed**
Jay S. **Duker**

ELSEVIER

Expert CONSULT Built with inkling | E books

Any screen. Any time. Anywhere.

Activate the eBook version
of this title at no additional charge.

Expert Consult eBooks give you the power to browse and find content, view enhanced images, share notes and highlights—both online and offline.

Unlock your eBook today.

1. Visit **expertconsult.inkling.com/redeem**
2. Scratch off your code
3. Type code into "Enter Code" box
4. Click "Redeem"
5. Log in or Sign up
6. Go to "My Library"

It's that easy!

Scan this QR code to redeem your eBook through your mobile device:

Place Peel Off Sticker Here

For technical assistance:
email expertconsult.help@elsevier.com
call 1-800-401-9962 (inside the US)
call +1-314-447-8200 (outside the US)

ELSEVIER

2015v1.0

ATLAS *of* RETINAL **OCT**

This page intentionally left blank

Atlas of Retinal OCT

Darin R. Goldman MD
Partner, Retina Group of Florida
Affiliate Associate Professor
Charles E. Schmidt College of Medicine
Florida Atlantic University
Boca Raton, FL, USA

Nadia K. Waheed MD, MPH
Assistant Professor of Ophthalmology
New England Eye Center
Tufts Medical Center
Tufts University School of Medicine
Boston, MA, USA

Jay S. Duker MD
Director, New England Eye Center
Professor and Chairman
Department of Ophthalmology
Tufts Medical Center
Tufts University School of Medicine
Boston, MA, USA

ELSEVIER

Edinburgh London New York Oxford Philadelphia St Louis Sydney Toronto

ELSEVIER

ISBN 978-0-323-46121-4
eISBN 978-0-323-46122-1

Notices

Knowledge and best practice in this field are constantly changing. As new research and experience broaden our understanding, changes in research methods, professional practices, or medical treatment may become necessary.

Practitioners and researchers must always rely on their own experience and knowledge in evaluating and using any information, methods, compounds or experiments described herein. Because of rapid advances in the medical sciences, in particular, independent verification of diagnoses and drug dosages should be made. To the fullest extent of the law, no responsibility is assumed by Elsevier, authors, editors or contributors for any injury and/or damage to persons or property as a matter of products liability, negligence or otherwise, or from any use or operation of any methods, products, instructions, or ideas contained in the material herein.

For Elsevier

Content Strategist: *Russell Gabbedy*
Content Development Specialist: *Joshua Mearns*
Project Manager: *Andrew Riley*
Designer/Design Direction: *Christian Bilbow*

Printed in China

Contents

Preface

Optical coherence tomography (OCT) continues to occupy an ever-expanding role in the ophthalmic community. OCT is widely available and forms a requisite portion of the comprehensive ophthalmic evaluation, particularly as it pertains to the retina. Although still a relatively young technology that continues to evolve, OCT has become widely accepted. This acceptance is due to its non-invasive nature, ease of image acquisition, and wealth of information that it affords. The quantity of information conveyed within a typical OCT scan is immense, which can be daunting to both the beginner and experienced clinician.

Atlas of Retinal OCT grew out of the success of *Handbook of Retinal OCT.* The Atlas expands on the images and material in the handbook, while maintaining a similar and consistent layout that will be familiar to the reader. This atlas was created to serve as a supplement to the original text, although the atlas certainly can stand alone as an independent reference. We sought to include a breadth of retinal conditions with a focus on those most applicable to everyday clinical practice. However, a wide array of pathology is included to also illustrate unique, less common OCT findings. Each condition is illustrated with numerous, large, high-quality OCT images to highlight disease pathology and aid in disease identification. Additional imaging modalities, such as fundus photographs and fluorescein angiograms, are included to supplement OCT images where appropriate.

Atlas of Retinal OCT provides the reader with a high quality, easy-to-follow visual aid to incorporating OCT scans into the evaluation and care of your patients. The atlas is designed to make OCT more comprehensible for both the novice and expert clinician. We hope that the reader finds this to be a handy and practical addition to your everyday reference armamentarium.

This page intentionally left blank

Contributors

A YASIN ALIBHAI, MD
OCT Research fellow, Ophthalmology, New England Eye Center, Tufts Medical Center, Boston, Massachusetts, USA

CAROLINE R. BAUMAL, MD
New England Eye Center, Tufts Medical Center, Boston, Massachusetts, USA

SHILPA DESAI, MD, FRCP
Assistant Professor, Ophthalmology, New England Eye Center/Tufts University Medical Center, Boston, MA, USA

IVANA N. DESPOTOVIC, MD
New England Eye Center, Tufts University School of Medicine, Boston, MA, USA

JAY S. DUKER, MD
Director, New England Eye Center, Professor and Chairman, Department of Ophthalmology, Tufts Medical Center, Tufts University School of Medicine, Boston, MA, USA

DANIELA FERRARA, MD, PhD
Assistant Professor of Ophthalmology, Tufts University School of Medicine, Boston, MA, USA

DARIN R. GOLDMAN, MD
Partner, Retina Group of Florida, Affiliate Associate Professor, Charles E. Schmidt College of Medicine, Florida Atlantic University, Boca Raton, FL, USA

NORA W. MUAKKASSA, MD
New England Eye Center, Tufts Medical Center, Hospital de Olhos do Paraná, Curitiba, Brazil

CARLOS A. MOREIRA NETO, MD, PhD
New England Eye Center, Tufts Medical Center, Hospital de Olhos do Paraná, Curitiba, Brazil

EDUARDO A. NOVAIS, MD
Department of Ophthalmology, Federal University of São Paulo, School of Medicine, São Paulo, Brazil

CARL REBHUN, BA
New England Eye Center, Tufts Medical Center, Tufts University School of Medicine, Boston, USA

LUIZ ROISMAN, MD
Department of Ophthalmology, Federal University of São Paulo, School of Medicine, São Paulo, Brazil

EDUARDO UCHIYAMA, MD
Retina Group of Florida, Boca Raton, FL, USA

NADIA K. WAHEED, MD, MPH
Assistant Professor of Ophthalmology, New England Eye Center, Tufts Medical Center, Tufts University School of Medicine, Boston, MA, USA

This page intentionally left blank

Acknowledgments

A project such as this requires contributions from many different groups and individuals to be successful. First and foremost, the images used in this atlas would not be possible without our many patients. We are very grateful to these individuals who trust their care in our hands on a daily basis. Additionally, we rely on the talented photographers and technical staff at both the New England Eye Center at Tufts Medical Center and Retina Group of Florida to obtain the majority of the included OCT images. Their expertise is reflected in the volume of high quality images available for inclusion in this project. We would also like to thank the many co-authors who have contributed to various chapters throughout the atlas. Additionally, thanks are due to our fellows whose archive of cases and interesting images were invaluable to this project. Specifically, we would like to thank Dr. Chris Or, who provided invaluable feedback on the final chapters. Lastly, the professionalism and expertise of the staff at Elsevier is unmatched. We want to thank the entire team at Elsevier who were critical to the completion of this project, in particular Russell Gabbedy, Humayra Rahman Khan, Joshua Mearns, and Andrew Riley.

Dedications

To the memory of my dear sister Candice, whose love, strength and determination live on in all that she touched. And to my daughter, Rona, who has added immeasurable joy to our lives.

D.R.G.

To Jujie, Memsie and Ammi, without whom none of this would have been possible.

N.K.W.

To my colleagues at the New England Eye Center who have assisted me in bringing innovation to eye care for over 3 decades.

J.S.D.

This page intentionally left blank

Normal Optic Nerve 1.1

Carlos A. Moreira Neto | Carl Rebhun

Spectral domain OCT (SD-OCT) devices have two scan patterns to analyze the optic nerve head (ONH): volume scans and line scans.

Volume Scans

Volume scans acquire a volumetric set of data, centered at the ONH. It delineates the optic disc margin and optic disc surface contour and is segmented to obtain the retinal nerve fiber boundaries. Each device has its own scanning protocol. The Cirrus HD-OCT identifies the center of the optic disc and creates a 3.46-mm circle on this location and calculates the thickness of the retinal nerve fiber layer (RNFL). The Heidelberg Spectralis creates a cylindrical volume with a diameter of 3.4 mm through and around the ONH (Duker, Waheed & Goldman 2014). The Optovue RTVue's protocol for the ONH consists of a grid pattern with circular and radial scans that acquires a 4- × 4-mm volume around the optic nerve. Because different machines use circles of different diameters around the center of the ONH, the measurement of RNFL between machines is not comparable (Duker et al. 2014).

Retinal Nerve Fiber Layer Thickness (RNFL)

OCT devices calculate RNFL thickness as the distance between the internal limiting membrane and the outer aspect of the RNFL (Fig. 1).

Ganglion Cell Complex

The ganglion cell complex (GCC) consists of the thickness of three inner retinal layers: the NFL, the ganglion cell layer, and the inner plexiform layer. The scan is centered at the fovea, and the software presents the results as a color-coded map, comparing to a normative database (Fig. 2).

Optic Nerve Morphology

SD-OCT devices also calculate optic nerve diameter, area, cup, and rim measurements (see Fig. 1). Each measurement varies according to age (Cavallotti et al. 2002) and ethnicity (Girkin 2008). According to Budenz et al. (2007), the mean RNFL thickness in a normal population is 100.1 μm. Thinner RNFL measurements were associated with older age. Caucasians had slightly thinner RNFL thickness than Hispanics or Asians. Persons with smaller optic disc areas also have thinner RNFL thickness.

Line Scans

Aiming to obtain a higher resolution visualization of structure and anatomic anomalies at the ONH, line scans provide a single or a series of high-resolution B-scans similar to the scans obtained in the macula (Fig. 3).

OCT angiography (OCTA) (Fig. 4) allowed for a greater understanding of optic disc vasculature and peripapillary vessel density. This information provides insight into the role of this vascular bed in the functioning of the RNFL.

REFERENCES

Budenz DL, Anderson DR, Varma R, et al. Determinants of normal retinal nerve fiber layer thickness measured by Stratus OCT. *Ophthalmology*. 2007;114(6):1046–1052.

Cavallotti C, Pacella E, Pescosolido N, et al. Age-related changes in the human optic nerve. *Can J Ophthalmol*. 2002;37(7):389–394.

Duker JS, Waheed NK, Goldman DR. *Scanning Principles. Handbook of Retinal OCT*. St Louis: Elsevier; 2014.

Girkin CA. Differences in optic nerve structure between individuals of predominantly African and European ancestry: Implications for disease detection and pathogenesis. *Clin Ophthalmol*. 2008;2(1):65–69.

ONH and RNFL OU Analysis: Optic Disc Cube 200×200 OD ● ○ OS

RNFL Thickness Map

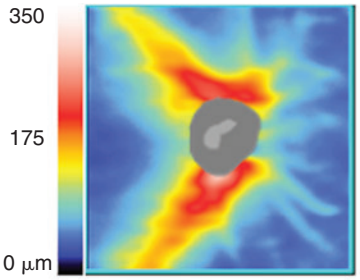

⚠	OD	OS
Average RNFL Thickness	102 µm	X
RNFL Symmetry	X	
Rim Area	1.88 mm^2	X
Disc Area	2.17 mm^2	X
Average C/D Ratio	0.36	X
Vertical C/D Ratio	0.32	X
Cup Volume	0.009 mm^3	X

RNFL Deviation Map

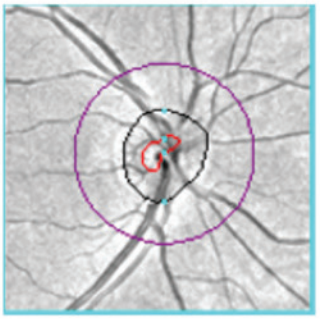

Disc Center (0.09,0.12) mm

Extracted Horizontal Tomogram

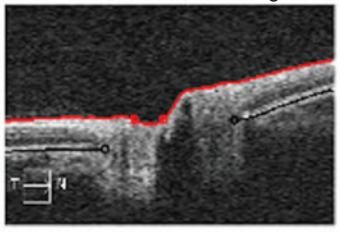

Extracted Vertical Tomogram

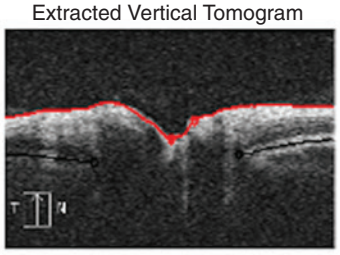

RNFL Circular Tomogram

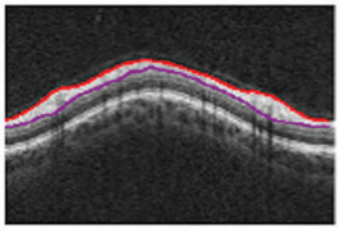

Neuroretinal Rim Thickness

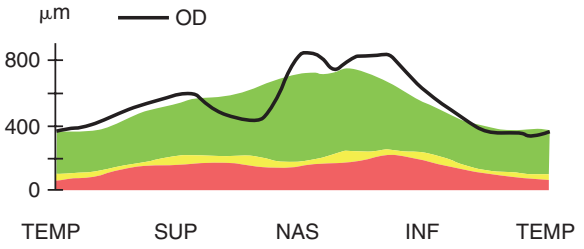

RNFL Thickness

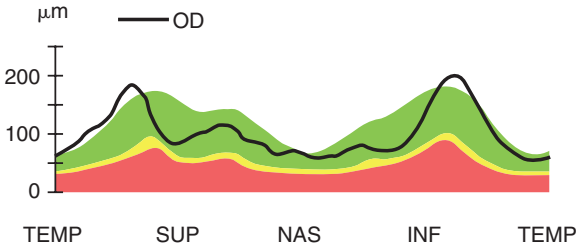

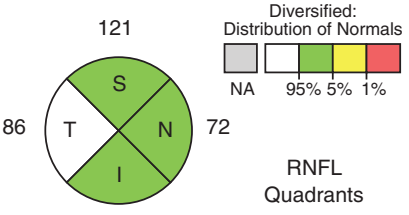

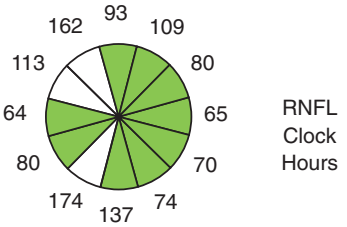

FIG. 1. Normal peripapillary RNFL, neuroretinal rim thickness, and disc area measurements using SD-OCT.

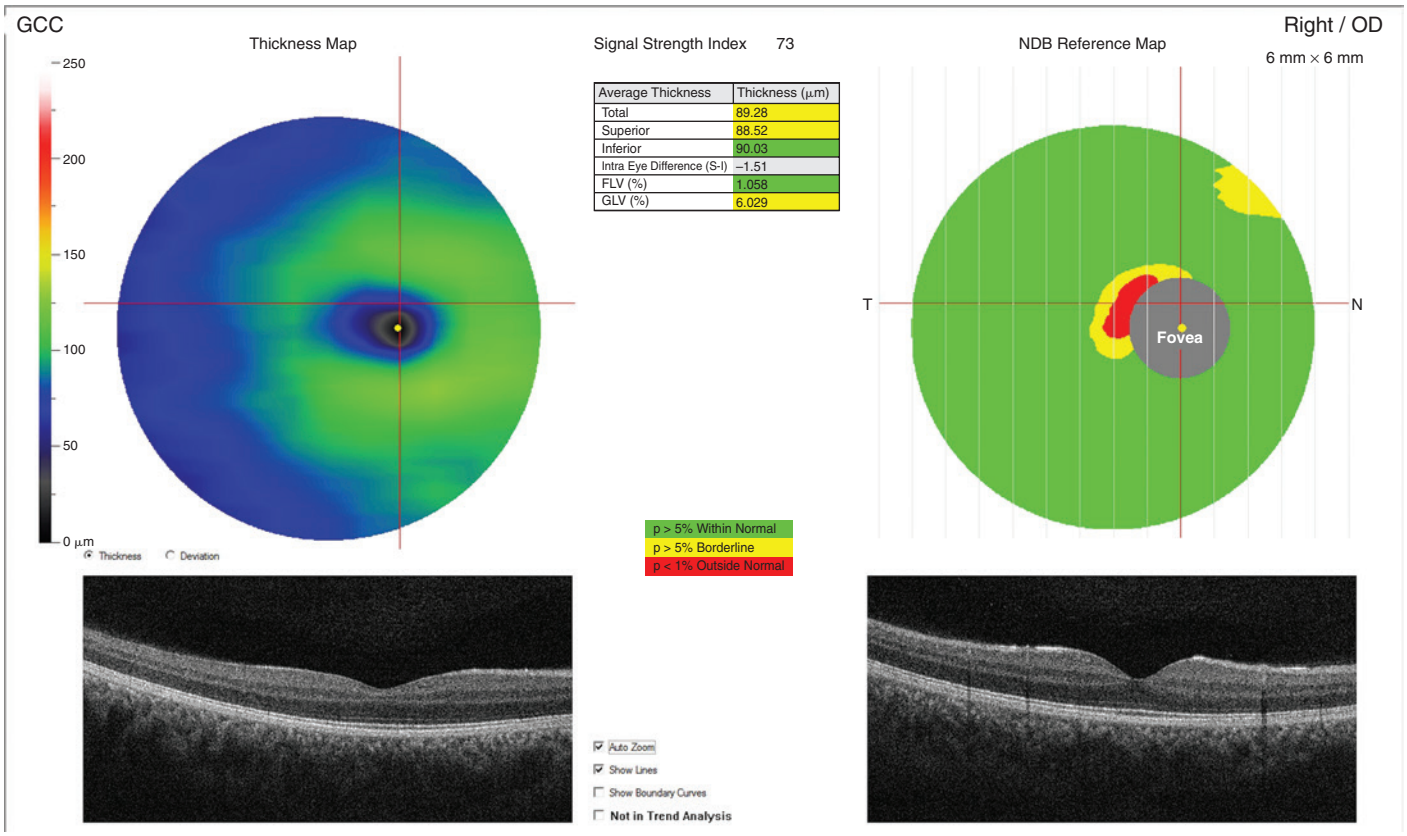

FIG. 2. Normal color-coded ganglion cell complex *(GCC)* thickness using SD-OCT.

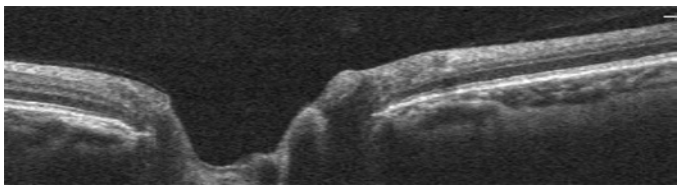

FIG. 3. Line scan of the ONH.

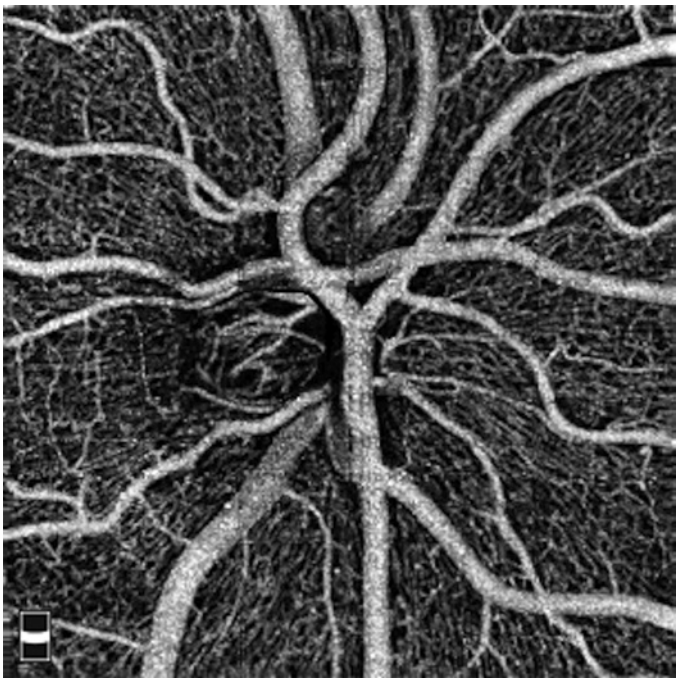

FIG. 4. OCT angiograph image (3 × 3 mm) of the ONH.

Time-Domain OCT

Carlos A. Moreira Neto | Carl Rebhun

2.1

The first OCT image, published by Huang et al. (1991), was captured using a device that detected light echoes using time domain detection. In time domain OCT (TD-OCT) the reference arm, with a physically moving mirror, and a sample arm undergo interference, which is used to generate an A-scan. Multiple A-scans obtained linearly are combined to generate a cross-sectional B-scan (Duker et al. 2014).

REFERENCES

Huang D, Swanson EA, Lin CP, et al. Optical coherence tomography. *Science*. 1991;254(5035):1178–1181.

Duker JS, Waheed NK, Goldman DR. Scanning principles. In: *Handbook of Retinal OCT*. St Louis: Elsevier; 2014.

Spectral Domain OCT

Carlos A. Moreira Neto | Carl Rebhun

2.2

Summary

In spectral domain OCT (SD-OCT), a spectral interference pattern between the reference beam and the sample beam is obtained simultaneously by a spectrometer and an array detector. Unlike time domain (TD)-OCT, SD-OCT does not require a physically moving reference mirror, instead using frequency information to produce interference patterns. This allows for much faster acquisition and higher quality images than those with TD-OCT.

The high resolution provided by SD-OCT allows for visualization of the microscopic anatomy of the retina (Fig. 1) with more detail than with TD-OCT.

Because the retinal pigment epithelium (RPE) is highly hyperreflective with OCT imaging, there is limited penetration of light beyond it, decreasing the resolution of the choroid (Schuman, Fujimoto & Duker 2013). Normal mean central foveal thickness is approximately 225 ± 17 μm as measured by SD-OCT, although this varies with age and retinal status.

REFERENCE

Schuman J, Fujimoto J, Duker J. *Optical Coherence Tomography of Ocular Diseases*. 3rd ed. Thorofare NJ: Slack Inc.; 2013.

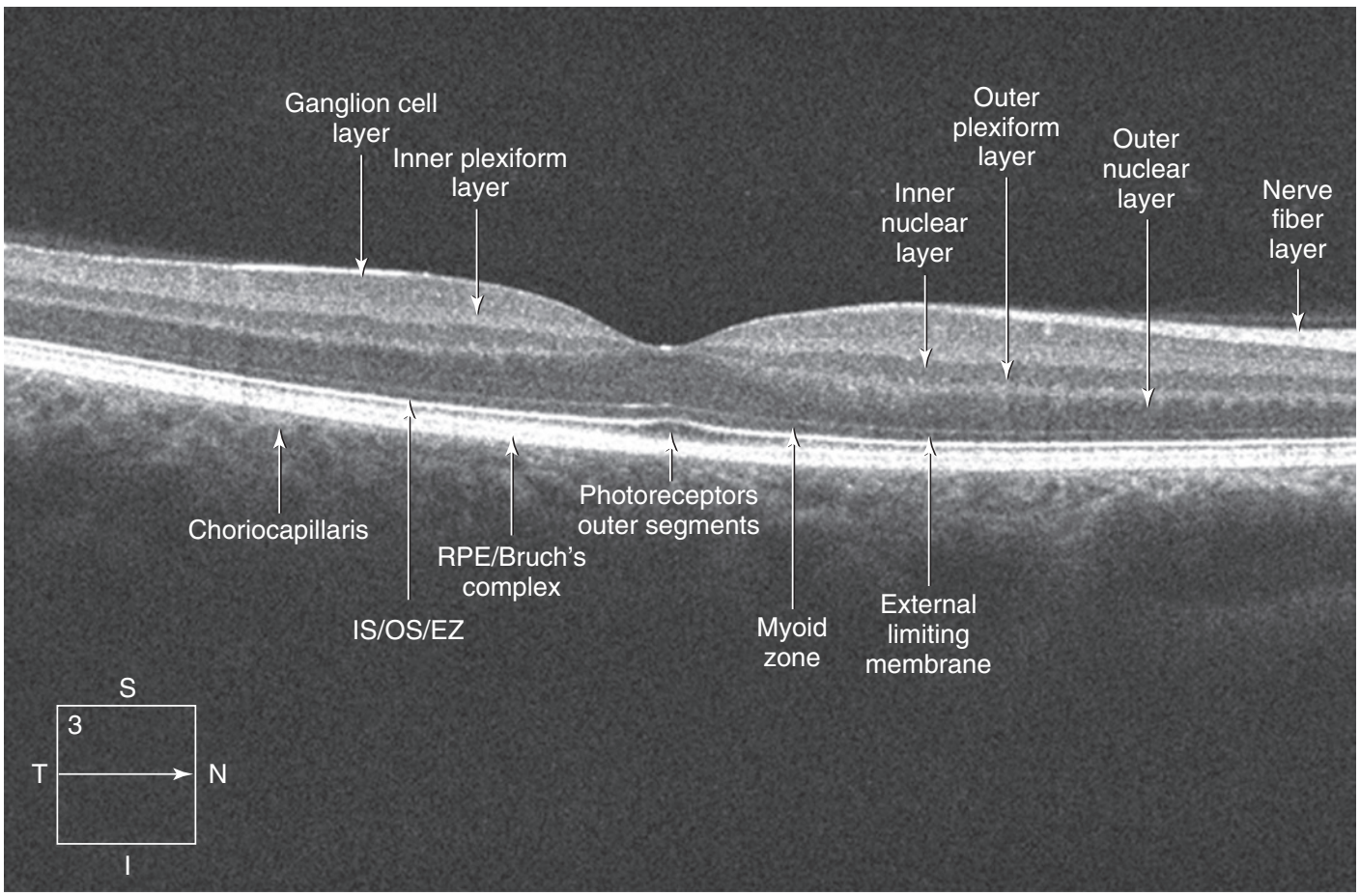

FIG. 1. Normal macula imaged using SD-OCT. *IS/OS/EZ,* Inner segment/outer segment/ellipsoid zone; *RPE,* retinal pigment epithelium.

Swept-Source OCT

Carlos A. Moreira Neto | Carl Rebhun

2.3

Summary

Swept source OCT (SS-OCT) is a modified Fourier-domain and depth-resolved technology that offers potential advantages over SD-OCT, including reduced sensitivity roll-off with imaging depth, higher detection efficiencies, improved imaging range, and better penetration of the choroid (Fig. 1). In SS-OCT, a narrow-band light source is rapidly swept through a wide range of frequencies. The interference pattern is detected on a single or small number of receivers as a function of time.

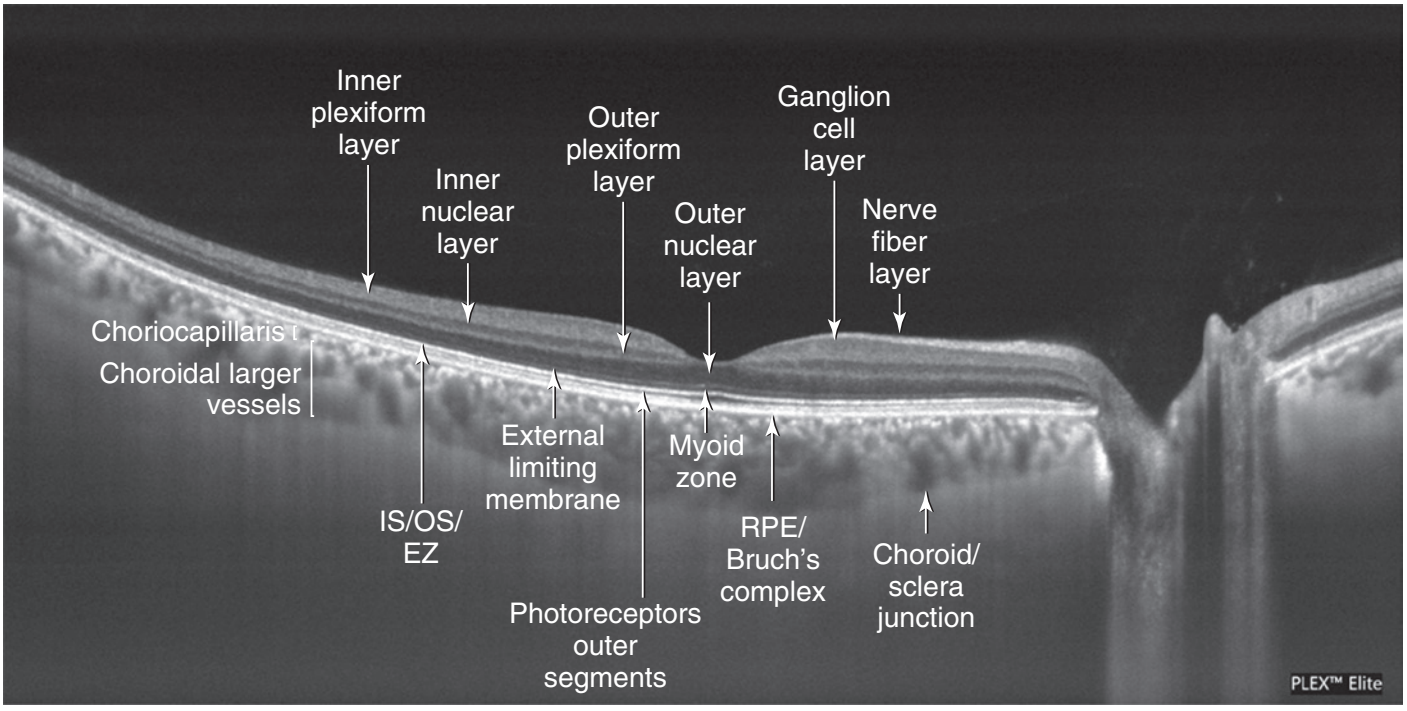

FIG. 1. Normal retina imaged using SS-OCT. EZ, ellipsoid zone; IS, inner segments; OS, outer segments; RPE, retinal pigment epithelium.

Normal Choroid 3.1

Carlos A. Moreira Neto | Carl Rebhun

Summary

Enhanced depth imaging (EDI) on commercially available OCT devices allows for higher quality images of the choroid (Fig. 1). EDI mode moves the zero-delay line of the spectral domain (SD)-OCT closer to the choroid, enabling better visualization of choroidal structures and a more precise measurement of choroidal thickness than standard OCT scanning protocols. This is useful for diseases such as central serous chorioretinopathy, in which the choroidal-scleral interface may be difficult to visualize. Studies of choroidal thickness in normal subjects and those with pathologic processes have shown a wide variation in measurements (Fujiwara et al. 2012; Margolis & Spaide 2009).

The choroid is divided into three layers, the choriocapillaris or smaller blood vessels, Sattler's layer, and Haller's layer, or larger blood vessels (Fig. 2).

REFERENCES

Margolis R, Spaide RF. A pilot study of enhanced depth imaging optical coherence tomography of the choroid in normal eyes. *Am J Ophthalmol*. 2009;147(5):811–815.

Fujiwara A, Shiragami C, Shirakata Y, et al. Enhanced depth imaging spectral-domain optical coherence tomography of subfoveal choroidal thickness in normal Japanese eyes. *Jpn J Ophthalmol*. 2012;56(3):230–235.

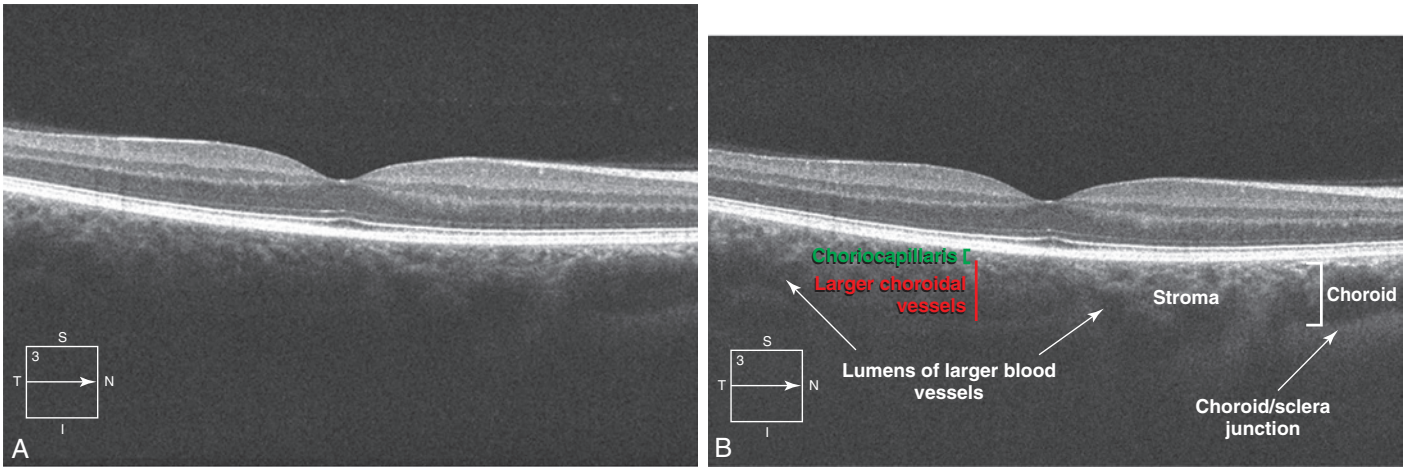

FIG. 1. Chorioretinal OCT image not using EDI (A) and using EDI (B).

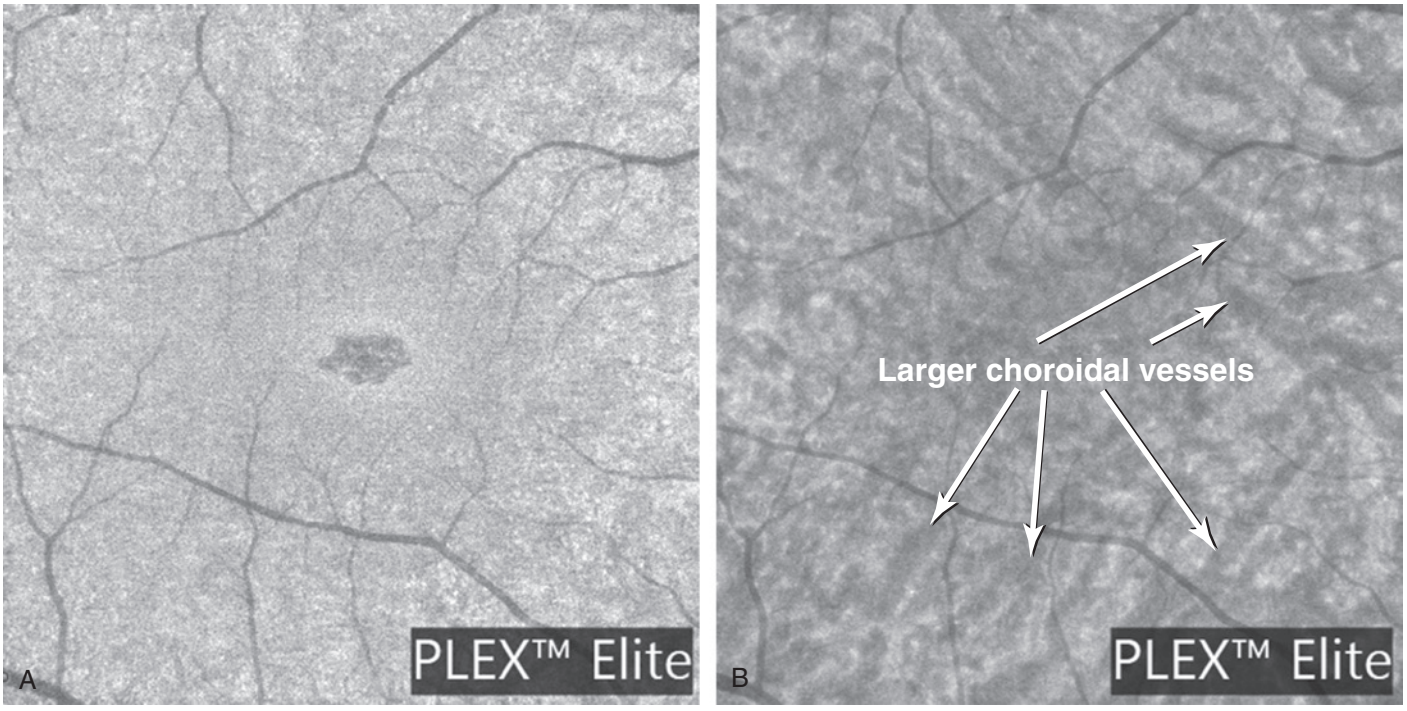

FIG. 2. En face structural OCT images of choriocapillaris (A) and Haller/Sattler layers (B).

Normal Vitreous 4.1

Nadia K. Waheed

Summary

Until recently, the anatomy of the vitreous could not be imaged in vivo. With the use of OCT, a better view and understanding of vitreous structure has become possible. Along with normal structure, abnormal vitreous processes such as vitreomacular traction have been revealed (Duker et al. 2013). High dynamic range imaging as well as enhanced vitreous imaging techniques, present on most commercially available OCT devices, allow visualization of the fluid-filled spaces as well as the collagenous and cellular structure of the vitreous. Secondary features of vitreous debris are also often identifiable on SD-OCT (Fig. 1).

Key OCT Features

In OCT of a normal retina the following vitreous structures may be observed:

- Posterior cortical vitreous (posterior hyaloid) (Fig. 2)
- Retrohyaloid space: Created after posterior vitreous detachment (Fig. 2).
- Premacular bursa: Liquid space overlying the macula, caused by liquefaction of the vitreous (Fig. 3).

REFERENCE

Duker JS, Kaiser PK, Binder S, et al. The International Vitreomacular Traction Study Group classification of vitreomacular adhesion, traction, and macular hole. *Ophthalmology*. 2013;120(12):2611–2619.

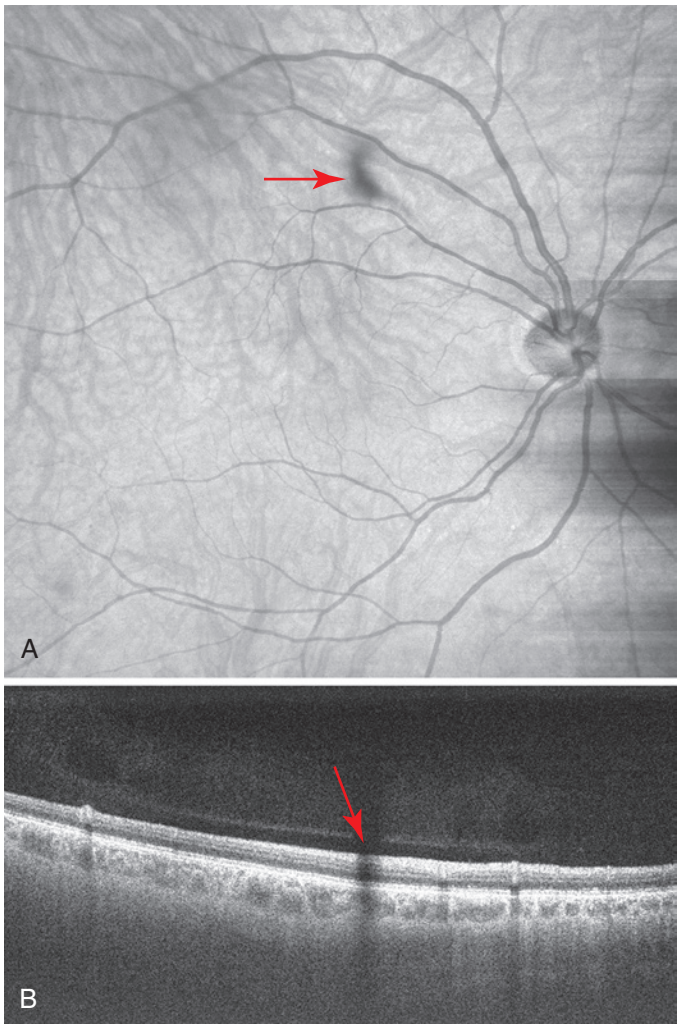

FIG. 1. Vitreous opacity *(arrows)* demonstrates shadowing on SS-OCT.

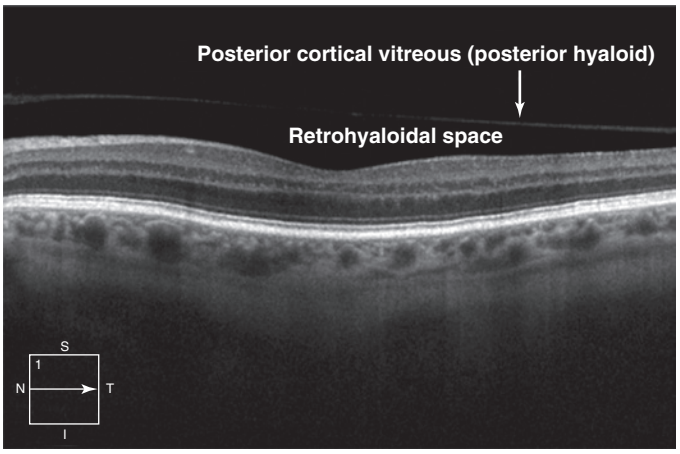

FIG. 2. Posterior hyaloid and retrohyaloid spaces.

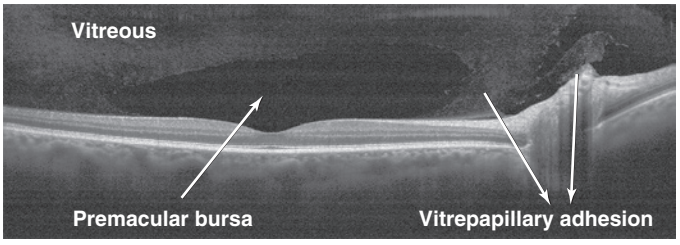

FIG. 3. Premacular bursa in a normal patient using SD-OCT.

OCT: Artifacts and Errors

Carlos A. Moreira Neto | Carl Rebhun

5.1

Artifacts can occur during image acquisition or analysis because of patient, operator, or software factors. Accurate image interpretation depends on the quality of the image and an understanding of the various artifacts that can affect an OCT image (Duker, Waheed & Goldman 2014).

Mirror Artifact

- Occurs only on spectral domain (SD)-OCT.
- Occurs when the area of interest crosses the zero-delay line and results in an inverted image.
- Reasons
  1. OCT device is pushed too close to the eye.
  2. Conditions in which the curvature of the retina is such that it crosses the zero-delay line, such as retinoschisis, retinal detachment, an elevated choroidal lesion, or high myopia (Fig. 1).

Vignetting

- Occurs when the iris blocks a part of the OCT beam.
- Loss of signal is seen over one side of the image (Fig. 2).

Misalignment

- This occurs when the fovea is not centered during the volumetric scan (Fig. 3).
- Most common reason is a patient with poor fixation or incorrect placement of fixation target by operator.

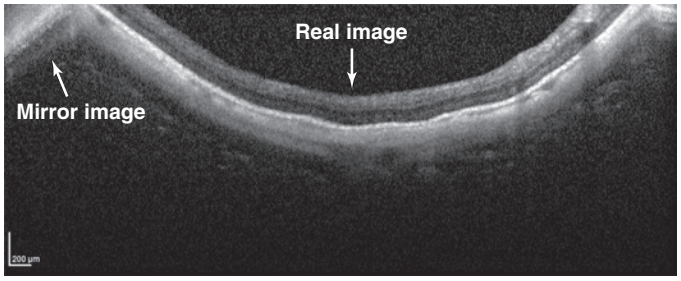

FIG. 1. Mirror artifact occurring in a high myopic eye.

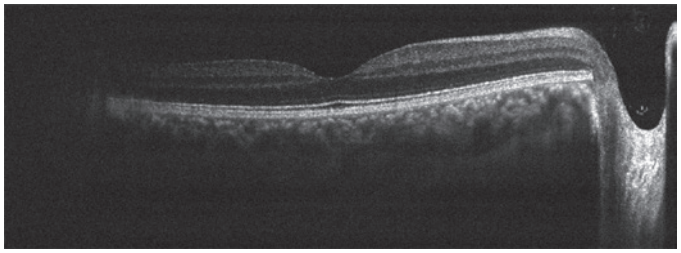

FIG. 2. Vignetting: Loss of signal over the left side of the image.

- The Early Treatment Diabetic Retinopathy Study (ETDRS) grid usually can be moved to obtain an accurate measure of the foveal thickness.

Software Breakdown

- OCT segmentation lines are incorrectly drawn because there is misidentification of the inner or outer retinal boundaries.
- Vitreomacular surface disorders (epiretinal membrane, vitreomacular traction) could cause inner line breakdown.
- Outer retinal/retinal pigment epithelium disorders (age-related macular degeneration, cystoid macular edema) might cause outer line breakdown (Fig. 4).

Blink Artifact

- If a patient blinks during image acquisition, loss of data occurs.
- OCT scans and volumetric maps both show black or white bars (Fig. 5).

Motion Artifact

- Occurs when there is movement of the eye during scan acquisition.
- OCT image shows distortion or double scanning of the same area.
- Blood vessels are misaligned (Fig. 6).
- The fovea may be duplicated.
- This is much less common due to better eye tracking software on current OCT machines.

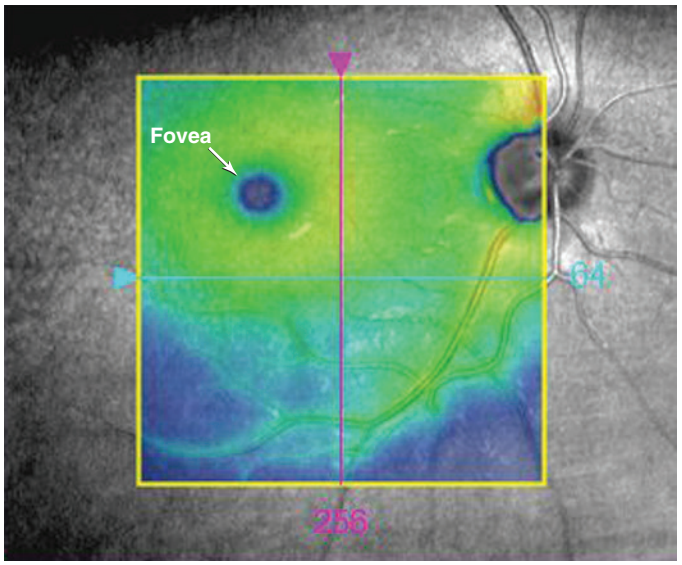

FIG. 3. Misalignment error. The fovea is not centered because of an eccentric fixation.

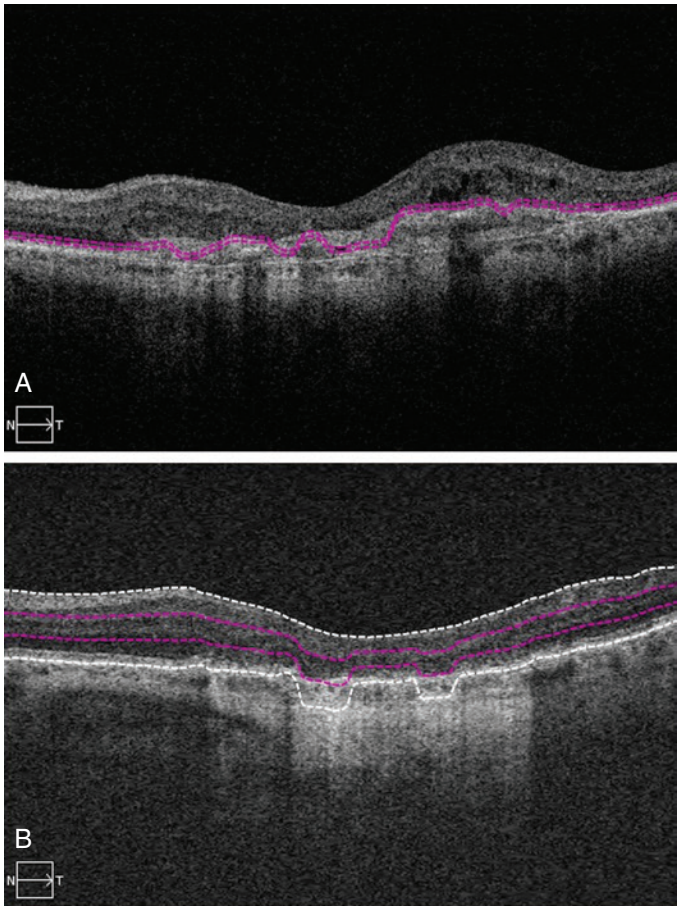

FIG. 4. Software breakdown caused by choroidal neovascularization (A) and geographic atrophy (B).

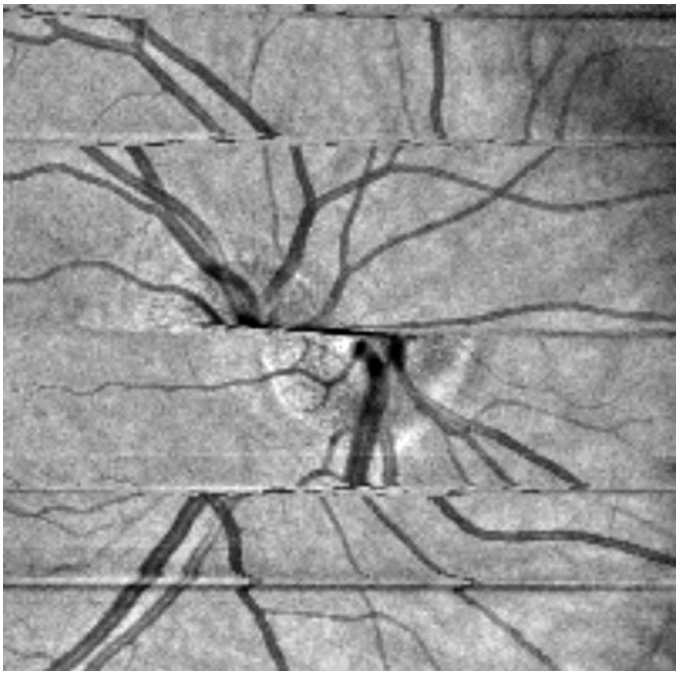

FIG. 6. Motion artifact.

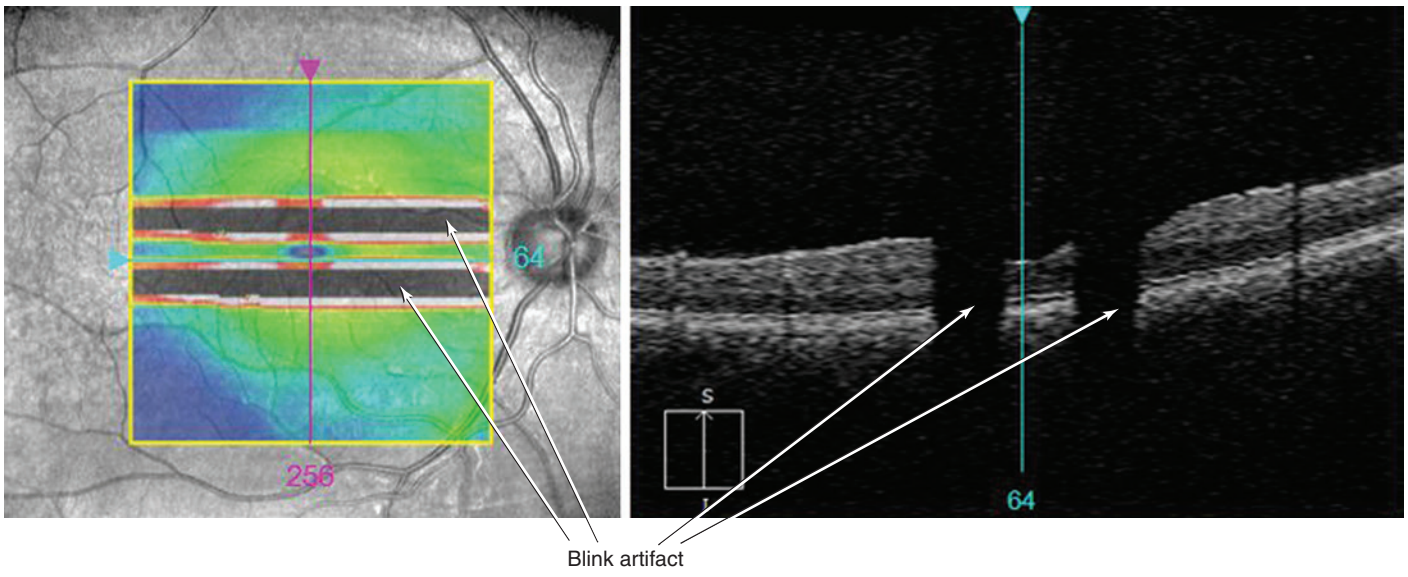

FIG. 5. Blink artifact.

Out of Range Error

- Occurs when the B-scan is not centered in the preview screen, resulting in it being shifted out of the scanning range.
- A section of the OCT scan is cut off (Fig. 7).

REFERENCE

Duker JS, Waheed NK, Goldman DR. *Artifacts on OCT. Handbook of Retinal OCT*. St Louis: Elsevier; 2014.

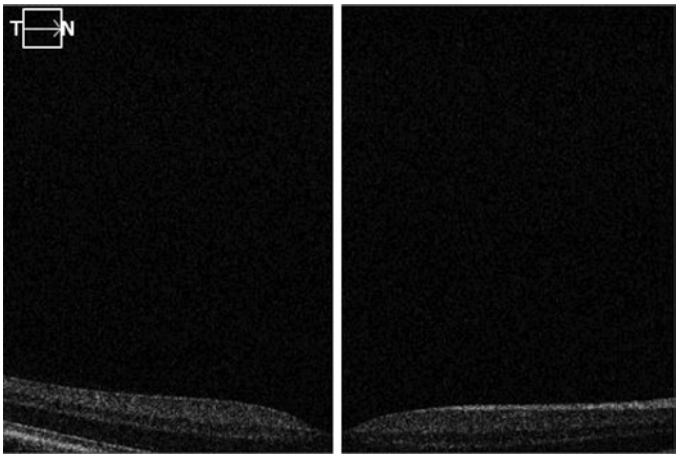

FIG. 7. Out-of-range error. Due to improper positioning of the machine during image acquisition, the outer retina and the choroid are cut off.

OCT Angiography Artifacts

Carlos A. Moreira Neto | Carl Rebhun

5.2

Artifacts are very common in OCT angiography, and their identification is important for appropriate image interpretation (Ferrara, Waheed & Duker).

Blockage Artifacts (Fig. 1)

- Blockage artifacts are caused by lesions that affect light penetration through ocular tissues, including both the anterior and posterior segments.
- Anterior segment blockage can be cause by cataract, inflammation, or corneal scar.
- Posterior segment blockage can be caused by intravitreal hemorrhage or inflammation, floaters, intraretinal or subretinal hemorrhage, pigment epithelial detachment (PED), or large drusen.

White Line Artifacts (Fig. 2)

- Caused by transverse ocular movements.
- A major cause of artifacts in OCT angiography.

False Positive Flow

- Ocular movements are in the axial direction (arterial pulsation).
- An OCT dataset may be displaced and may have enough decorrelation to cause the appearance of flow (Ferrara, Waheed & Duker 2016; Spaide, Fujimoto & Waheed 2015).

Quilting Defects (Fig. 3)

- Related to software correction of ocular movement.
- Caused by multiple saccades in the horizontal and vertical directions.

False Negative Flow

- Caused by blood flow below a given threshold.
- Vessels seem absent even if they are present.

Projection Artifacts (Fig. 4)

- Superficial vessels are seen in deep and choroidal slabs when they are not actually present in those slabs (Ferrara et al. 2016; Spaide et al. 2015).

Vessel Duplication (Fig. 5)

- Result of a breakdown in registration of the X and Y scans.
- Caused by eye movement.

Segmentation Errors (Fig. 6)

- Caused by PED, macular edema, or other pathologic process that disrupts the horizontal alignment of retinal layers.

Shadowing Artifacts (Fig. 7)

- Usually appear in choriocapillary segmentation.
- Caused by PED, hemorrhage, floaters.

REFERENCES

Ferrara D, Waheed NK, Duker JS. Investigating the choriocapillaris and choroidal vasculature with new optical coherence tomography technologies. *Prog Retin Eye Res*. 2016;52:130–155.

Spaide RF, Fujimoto JG, Waheed NK. Image Artifacts in Optical Coherence Tomography Angiography. *Retina*. 2015;35(11):2163–2180.

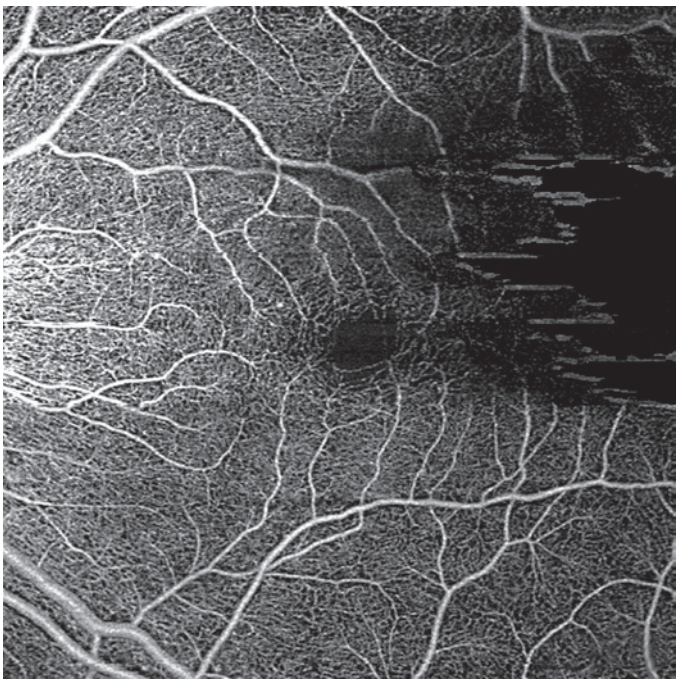

FIG. 1. Blockage artifact causing a focal loss of signal.

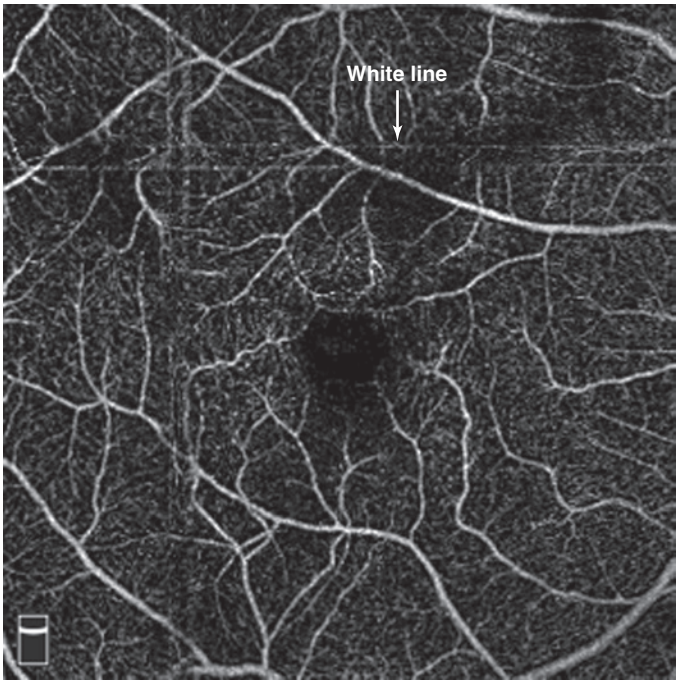

FIG. 2. White line artifact.

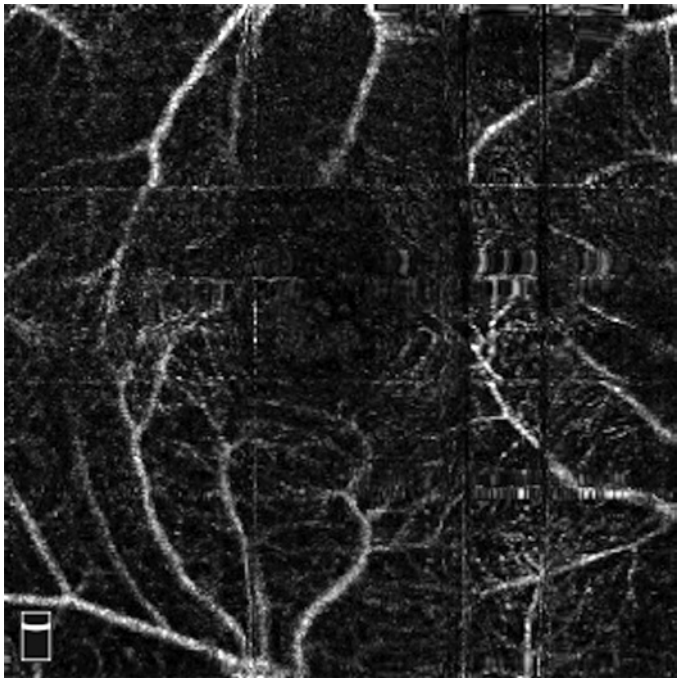

FIG. 3. Quilting artifact.

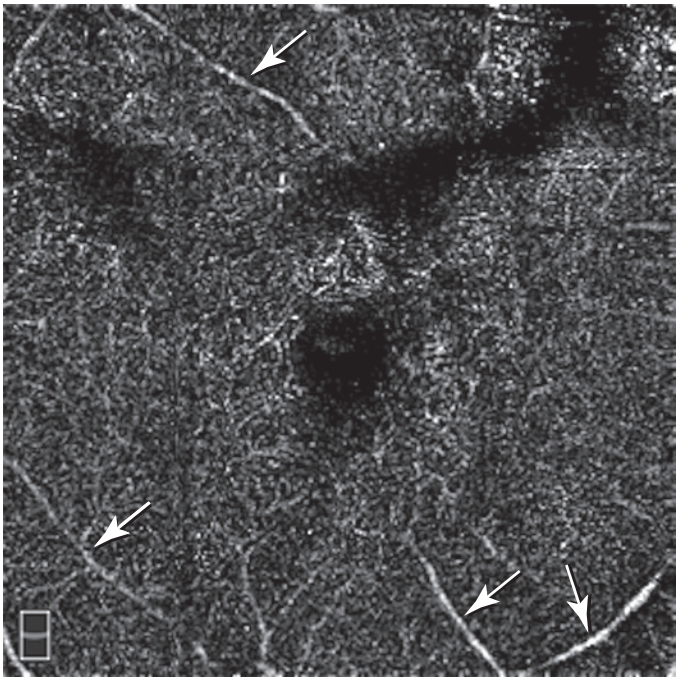

FIG. 4. Projection artifact on deep plexus. Vessels from the superficial plexus *(arrows)* are seen in the deep plexus.

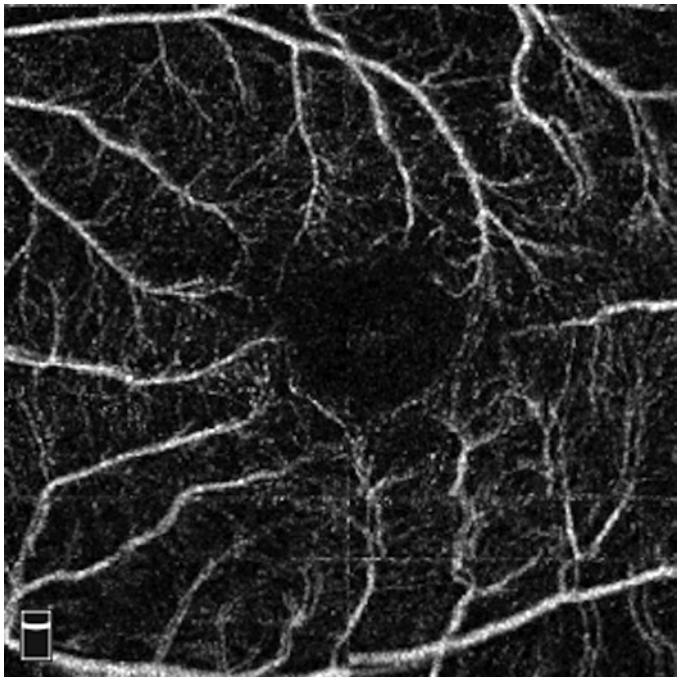

FIG. 5. Vessel duplication.

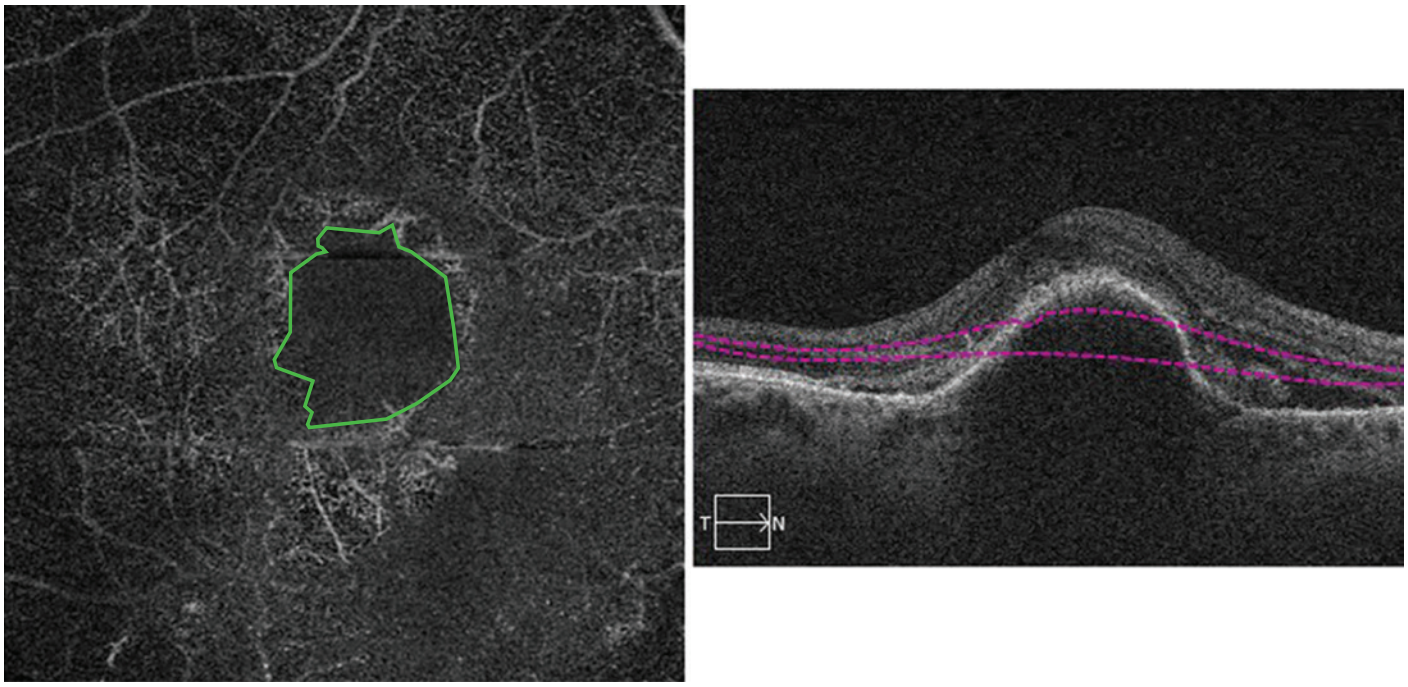

FIG. 6. Segmentation error *(green line)* caused by a pigment epithelial detachment.

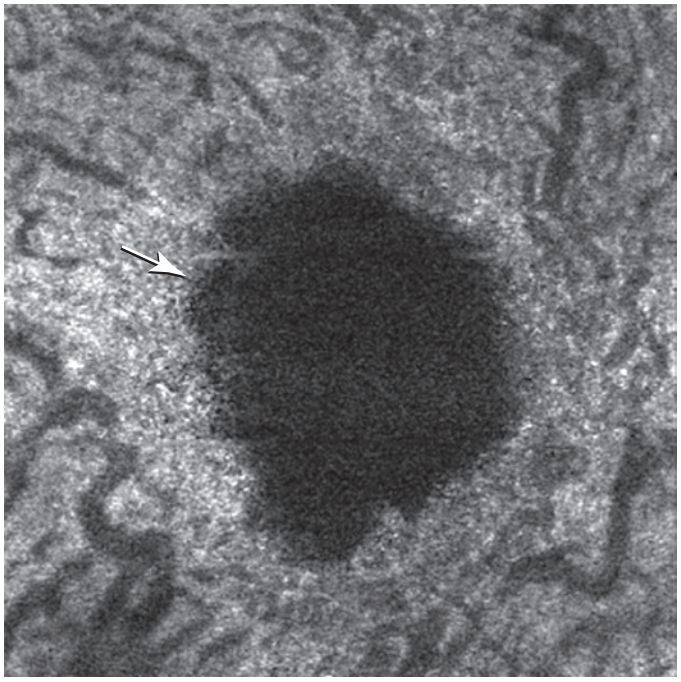

FIG. 7. Shadowing artifact *(arrow)* in the choriocapillaris segmentation.

Drusen

Ivana N. Despotovic | Daniela Ferrara

6.1.1

Summary

Drusen are focal yellow or white deposits of extracellular debris located between the retinal pigment epithelium (RPE) and Bruch's membrane. They occur naturally with age and usually are asymptomatic. Drusen are the hallmark of age-related macular degeneration (AMD) and the most common early sign of nonexudative AMD. Esterified and unesterified cholesterol are significant components of the lipid-rich lesions associated with AMD (basal linear deposits and soft drusen) and comprise more than 40% of hard druse volume (Curcio et al. 2011).

Drusen may range in appearance, size, and location. Hard drusen are smaller and have distinct margins (Figs. 2, 3, 4, 5, 6, 10, and 12). Soft drusen are larger, mound-like elevations that may have a diameter greater than 1000 µm, with margins that are not clearly defined (Figs. 1, 2, 3, 4, 7, 8, 9, and 11). A large number of round and punctate cuticular drusen give a "stars in the sky" appearance. Cuticular drusen have a spheroid or triangular shape on OCT (Fig. 12).

The tomographic features of drusen on OCT have been extensively investigated in natural history studies as potential biomarkers for AMD progression, although some features have yet to be validated. Among drusen characteristics defined on cross-sectional OCT, drusen shape, internal reflectivity, and substructures can be cited as some of the relevant biomarkers with increased risk for development to advanced AMD (Yehoshua et al. 2011; Veerappan et al. 2016). Drusen size and confluency have been historically associated with the progression of AMD. More recently, drusen volume has been assessed through automatic OCT algorithms, which also appears to be relevant in disease progression (Abdelfattah et al. 2016).

Drusenoid pigment epithelial detachment (PED) is formed by the confluence of large areas of soft drusen (Figs. 7, 8, and 11) and is part of the clinical spectrum of AMD (Casswell, Kohen, & Bird 1985). The natural history of eyes containing drusenoid PED is characterized by a high rate of progression to both geographic atrophy (GA) and neovascular AMD (Cukras et al. 2010).

Subretinal drusenoid deposits (SDDs, also known as reticular pseudodrusen, can be confounded with drusen, but are actually a clinically distinct entity located above the RPE (Figs. 3, 4, and 10). OCT is considered a fundamental imaging modality to identify and characterize SDD (Suzuki, Sato & Spaide 2014; Zweifel et al. 2010). SDD in older eyes with a normal macular appearance, as defined by the Age-Related Eye Disease Study (AREDS) scale, is a risk factor for further development of AMD (Huisingh et al. 2016). Reduced visibility of cones overlying SDD in adaptive optics images can be due to several possible causes, including a change in photoreceptors' orientation, an alteration of their cellular architecture, or absence of the cones themselves, implying decreased cone photoreceptor function (Mrejen et al. 2014).

OCT imaging of refractile drusen (drusenoid material containing small refractile spherules) show hyperreflective dots (many small spherules rich in calcium phosphate) and appear to be a stage of drusen regression marked by loss of RPE, thus contributing to the development of GA (Suzuki et al. 2015).

Key Points

- Small drusen ("drupelets") are less than 63 µm in diameter, intermediate drusen are 63 to 125 µm, and large drusen are greater than 125 µm.
- Small drusen are considered normal aging and do not represent a risk for progression to advanced AMD.
- Subretinal drusenoid deposits (also known as reticular pseudodrusen) are located above the RPE and are associated with progression to advanced AMD.
- OCT is valuable in the differential diagnosis of drusen.
- Specific drusen features on OCT are investigated as biomarkers for AMD progression.

REFERENCES

Abdelfattah NS, Zhang H, Boyer DS, et al. Drusen volume as a predictor of disease progression in patients with late age-related macular degeneration in the fellow eye. *Invest Ophthalmol Vis Sci*. 2016;57(4):1839–1846.

Casswell AG, Kohen D, Bird AC. Retinal pigment epithelial detachments in the elderly: classification and outcome. *Br J Ophthalmol*. 1985;69(6):397–403.

Cukras C, Agrón E, Klein ML, et al. Age-Related Eye Disease Study Research Group. Natural history of drusenoid pigment epithelial detachment in age-related macular degeneration: Age-Related Eye Disease Study Report No. 28. *Ophthalmology*. 2010;117(3):489–499. doi:10.1016/j.ophtha.2009.12.002.

Curcio CA, Johnson M, Rudolf M, et al. The oil spill in ageing Bruch membrane. *Br J Ophthalmol*. 2011;95(12):1638–1645. doi:10.1136/bjophthalmol-2011-300344.

Huisingh C, McGwin G Jr, Neely D, et al. The Association between subretinal drusenoid deposits in older adults in normal macular health and incident age-related macular degeneration. *Invest Ophthalmol Vis Sci*. 2016;57(2):739–745. doi:10.1167/iovs.15-18316.

Mrejen S, Sato T, Curcio CA, et al. Assessing the cone photoreceptor mosaic in eyes with pseudodrusen and soft Drusen in vivo using adaptive optics imaging. *Ophthalmology*. 2014;121(2):545–551. doi:10.1016/j.ophtha.2013.09.026. [Epub 2013 Oct 30].

Suzuki M, Curcio CA, Mullins RF, et al. Refractile Drusen: Clinical imaging and candidate histology. *Retina*. 2015;35(5):859–865. doi:10.1097/IAE.0000000000000503.

Suzuki M, Sato T, Spaide RF. Pseudodrusen subtypes as delineated by multimodal imaging of the fundus. *Am J Ophthalmol*. 2014;157(5):1005–1012.

Veerappan M, El-Hage-Sleiman AM, Chiu SJ, et al. Optical coherence tomography reflective drusen substructures predict progression to geographic atrophy in age-related macular degeneration. *Ophthalmology*. 2016;123(12):2554–2570.

Yehoshua Z, Wang F, Rosenfeld PJ, et al. Natural history of drusen morphology in age-related macular degeneration using spectral domain optical coherence tomography. *Ophthalmology*. 2011;118(12):2434–2441.

Zweifel SA, Spaide RF, Curcio CA, et al. Reticular pseudodrusen are subretinal drusenoid deposits. *Ophthalmology*. 2010;117(2):303–312.

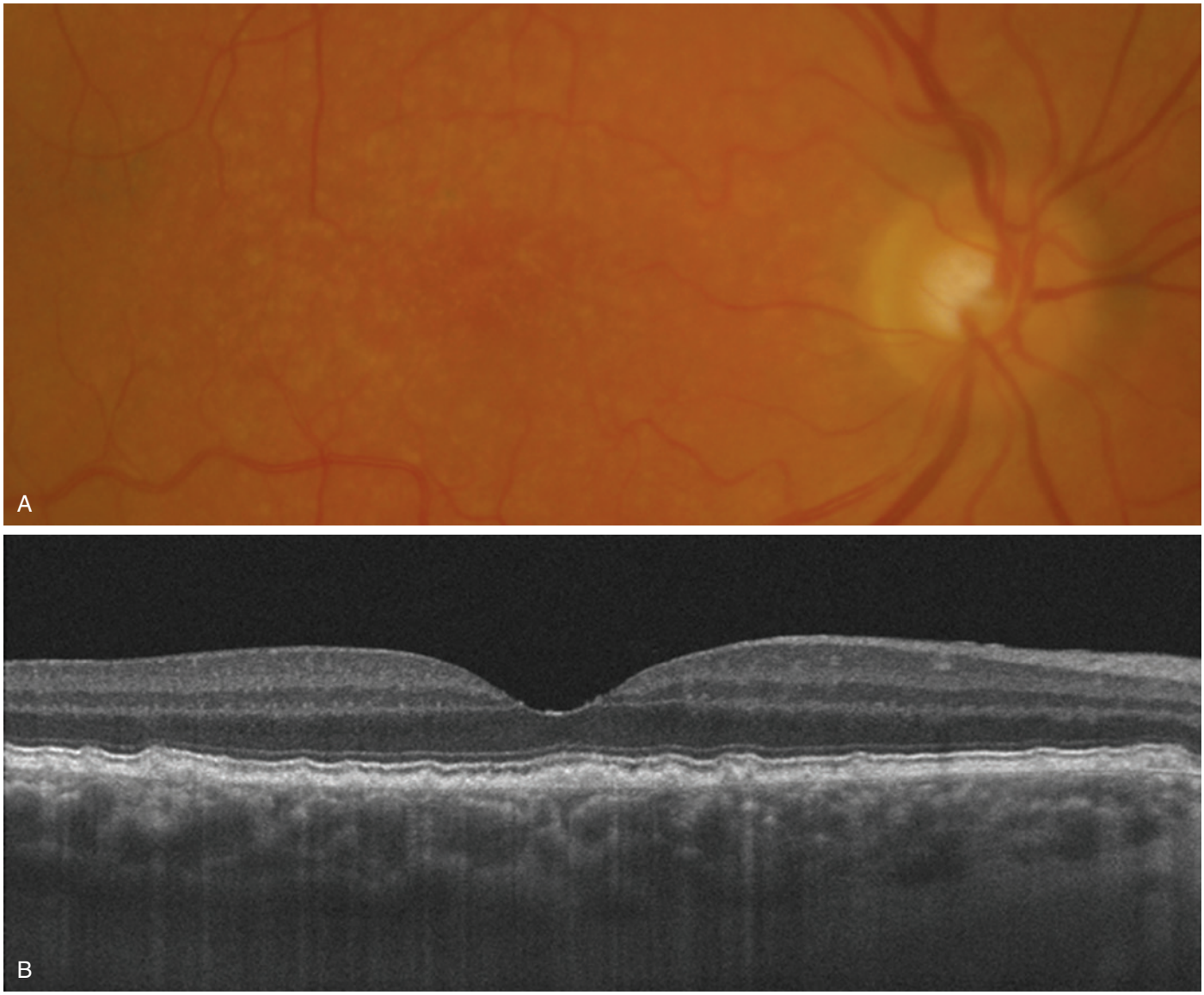

FIG. 1. (**A**) Color fundus photograph of soft drusen with indistinct margins. (**B**) Cross-sectional OCT B-scan shows soft drusen.

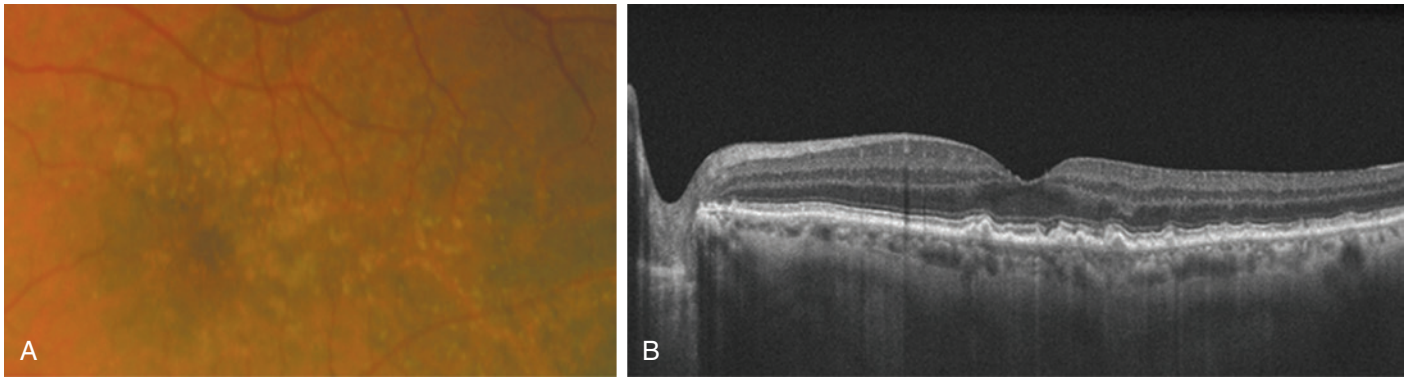

FIG. 2. (**A**) Color fundus photograph of multiple large soft drusen and distinct small hard drusen. Reticular pseudodrusen are present in the superior portion on the macula. (**B**) OCT B-scan shows confluent soft drusen and a few hard drusen.

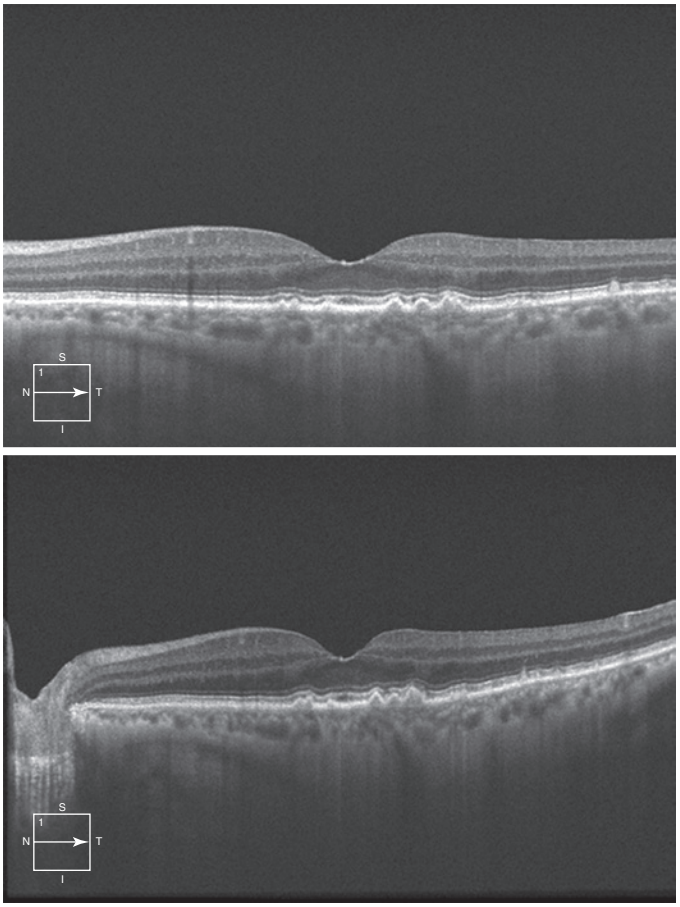

FIG. 3. OCT B-scans of the same eye depicted in Fig. 2. Reticular pseudodrusen are evident on the *right side* of the scans, in addition to confluent soft drusen and a few hard drusen, that are also visible in Fig. 2.

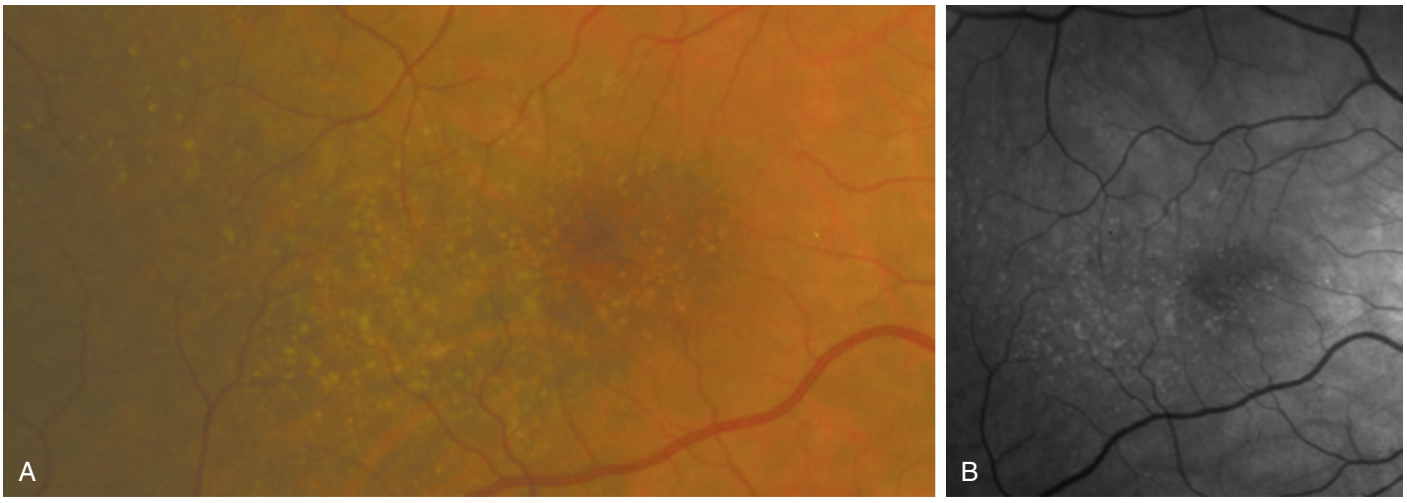

FIG. 4. (**A**) Color fundus photograph showing hard and soft drusen, as well as reticular pseudodrusen. (**B**) Red-free fundus photograph of the same eye.

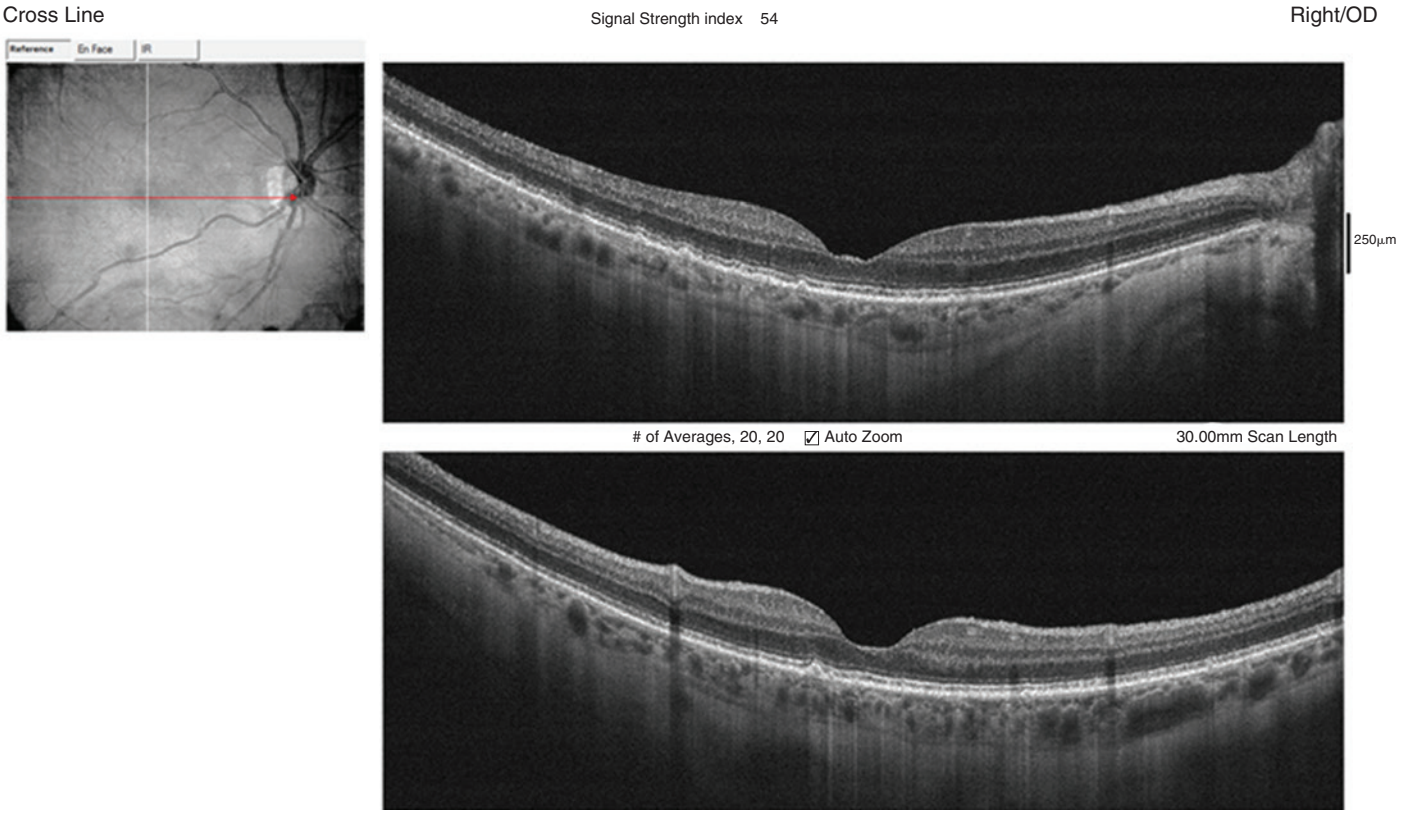

FIG. 5. En face and cross-sectional wide-field OCT B-scan of the same eye depicted in Fig. 4, showing distinct drusen.

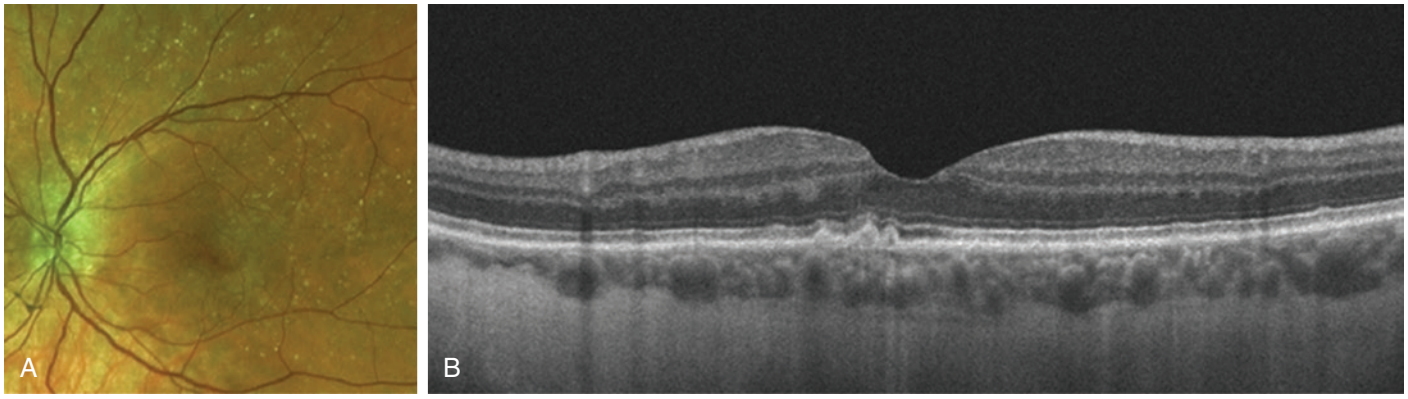

FIG. 6. (**A**) Color fundus photograph showing hard and soft drusen. (**B**) OCT B-scan shows hard and soft drusen.

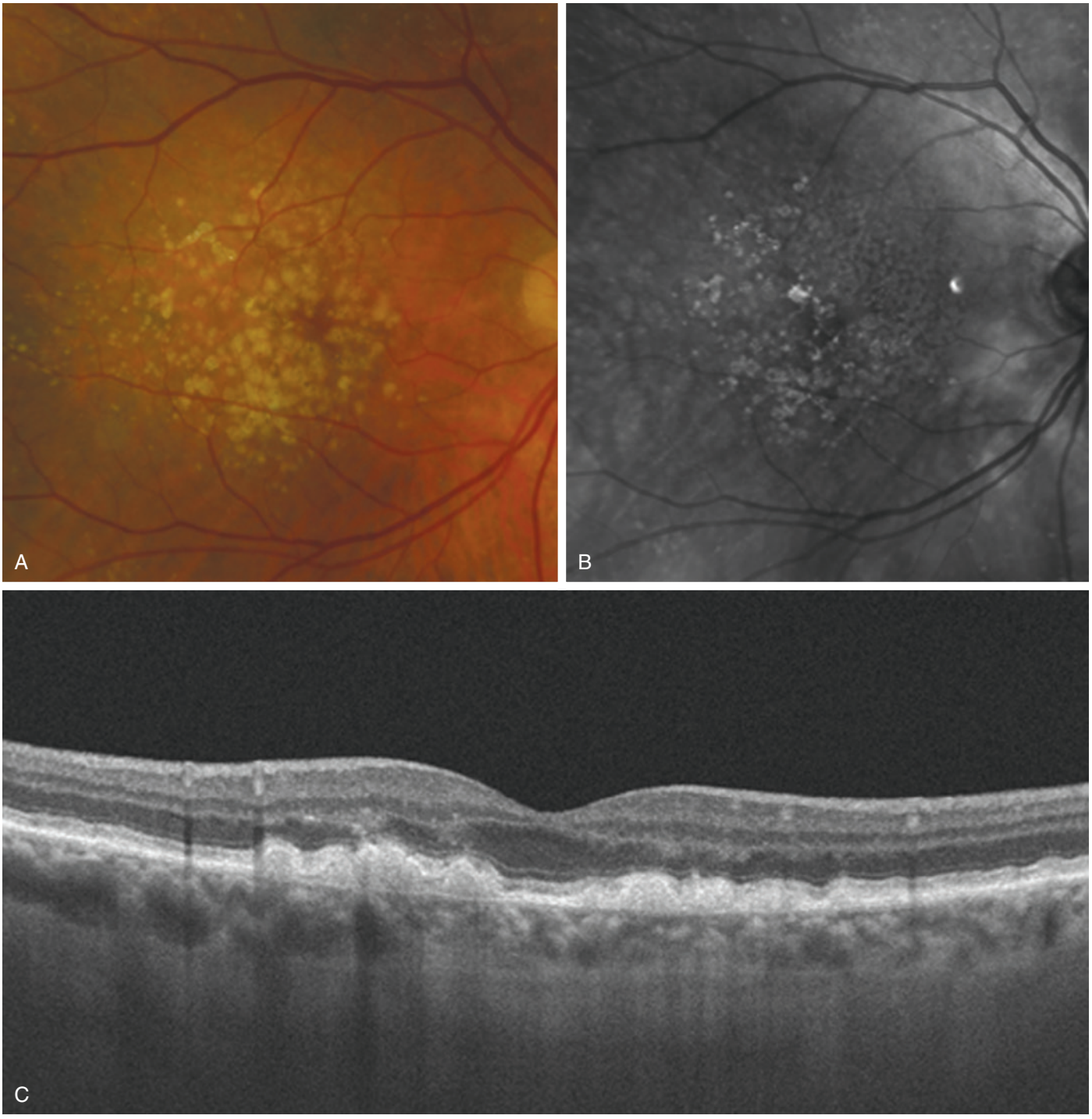

FIG. 7. (**A**) Color fundus photograph of multiple, confluent, large, soft drusen. (**B**) Near-infrared imaging of the same eye. (**C**) OCT B-scan shows confluent soft drusen and a drusenoid pigment epithelium detachment.